Ohyung Kwon, Hyun Sook Bae, and Ki-Woong Whang

Discharge characteristics of He–Ne–Xe gas mixture with varying Xe contents and at varying sustain electrode gap lengths in the plasma display panel

Ohyung Kwon,[1] Hyun Sook Bae,[2] and Ki-Woong Whang[1,a]

[1]*Plasma Laboratory, Inter-University Semiconductor Research Center, Department of Electrical and Computer Engineering, College of Engineering, Seoul National University, Seoul 151-742, Republic of Korea*
[2]*Information & Electronics Research Institute, School of Electrical Engineering and Computer Science, Korea Advanced Institute of Science and Technology, Daejon 305-701, Republic of Korea*

The discharge characteristics of He–Ne–Xe gas mixture in the plasma display panel were investigated using a two-dimensional numerical simulation to understand the effects of adding He and varying the Xe contents in the gas mixture, and also varying sustain electrode gap. With 5% Xe content and 60 μm sustain electrode gap, decreased ionization led to the improvement of the vacuum ultraviolet (vuv) efficacy at increasing He mixing ratios. However, at 20% Xe content and 60 μm sustain electrode gap, increased electron heating improved the vuv efficacy until the He mixing ratio reached 0.7, but the efficacy decreased beyond the ratio of 0.7 due to the increased ionization of Xe atoms. At 5% Xe content and 200 μm sustain electrode gap, the vuv efficacy increased as a result of increased electron heating at the gap space at increasing He mixing ratios. © 2009 American Institute of Physics. [doi:10.1063/1.3224960]

I. INTRODUCTION

Currently, the plasma display panel (PDP) is one of the most favored display devices in the large-sized panel market, but they need an improved luminous efficacy in order to satisfy energy conscious consumers. It has been reported that the luminous efficacy can be improved by using discharge gas with high Xe content[1–3] or a cell structure with a long sustain electrode gap.[4] The mechanism for improving the luminous efficacy, by application of high Xe contents and long sustain electrode gap together, has been investigated previously.[5] It has also been reported that the addition of He to the usual Ne–Xe gas mixture is effective in improving the luminous efficacy.[6,7]

In this paper, the mechanism of the efficacy improvement by the addition of He gas to the Ne–Xe mixture has been investigated via a two-dimensional numerical simulation study. The local field approximation and drift-diffusion approximation are assumed to solve the momentum equation. There are six different types of ions in the model: He^+, He_2^+, Ne^+, Ne_2^+, Xe^+, and Xe_2^+. The excited states of He and Ne are He^* (lumped $^3S_1$, $^1S_0$, $^3P_2$, $^3P_1$, $^3P_0$), He^{**} (lumped $^1P_1$, $\geq 3s$), Ne^* (lumped $^3P_2$, $^3P_1$, $^1P_1$), Ne^{**} (lumped $\geq 3p$), and Ne_2^* (lumped $^3\Sigma_u^+$, $^3\Sigma_g^+$, $^1\Sigma_u^+$, $^1\Sigma_g^+$); and the excited states of Xe are $Xe^*(^3P_2)$, $Xe^*(^3P_1)$, Xe^{**} (lumped $^3P_0$, $^1P_1$, $\geq 6p$), $Xe^{**}(O_u^+)$, and Xe_2^* (lumped $^3\Sigma_u^+$, $^1\Sigma_u^+$). The detailed description of the numerical simulation has been reported elsewhere.[8] The secondary electron emission coefficients, which are taken from Ref. 9, are 0.3 for He^+, He_2^+, 0.2 for Ne^+, Ne_2^+ and 0.02 for Xe^+, Xe_2^+.

Figure 1 shows a cross-section view of the PDP cell used in the numerical simulation where the cell pitch is 810 μm and the barrier rib height is 140 μm. A dielectric layer of 30 μm thickness covers the sustain electrode, and a 20 μm dielectric layer and 10 μm phosphor layer cover the address electrode in the rear plate. The width of the sustain electrode is fixed at 260 μm and effects of the He addition to the Ne–Xe mixture with the simultaneous change in the electrode gap from 60 to 200 μm or the Xe content from 5% to 20% have been studied. The sustain voltage used in this simulation is the median value of the minimum and maximum sustain voltage for each gas and sustain electrode gap condition.

II. RESULTS AND DISCUSSION

Figure 2 shows the vacuum ultraviolet (vuv) efficacy and the vuv output with the He addition in Ne–Xe mixtures and at 60 and 200 μm sustain electrode gap. The vuv efficacies at both 60 and 200 μm sustain electrode gap increase with increasing He mixing ratio at the fixed 5% Xe content. However, at 20% Xe content and 60 μm sustain electrode gap, the vuv efficacy increases until the He mixing ratio of 0.7, and then decreases beyond that. As the He mixing ratio increases, the vuv output at 5% Xe content and 60 μm sustain electrode gap increases, but it decreases after the He mixing ratio of 0.5 is reached. The vuv output at 5% Xe content and 200 μm sustain electrode gap increases with increasing He
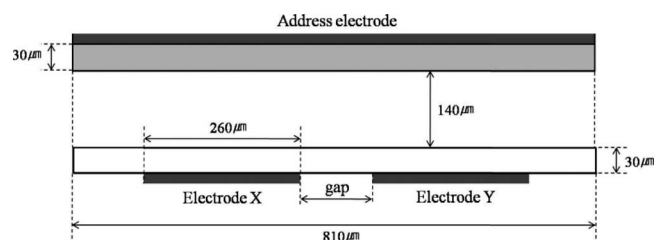

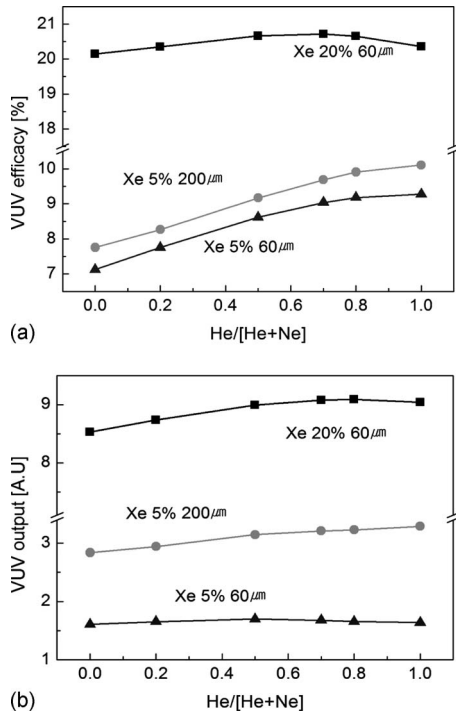FIG. 1. Cross-section view of PDP cell.

a)Electronic mail: kwhang@sun.ac.kr.

FIG. 2. (a) vuv efficacy and (b) vuv output at increasing He mixing ratios at 5% Xe content and 60 μm electrode gap, 5% Xe content and 200 μm electrode gap, and 20% Xe content and 60 μm electrode gap.

FIG. 3. Mobility of ion species at increasing He mixing ratios at (a) 5% Xe content and (b) 20% Xe content.

mixing ratio. The vuv output at 20% Xe content and 60 μm sustain electrode gap increases until the He mixing ratio becomes 0.8 and then decreases beyond that. These simulation results agree well with the experimental results reported by other research groups.[6,10] As we can see from these results, there are optimum He addition ratios to the Ne–Xe mixture for the improvement of luminous efficacy with changing Xe content and electrode gap. Now, the physical mechanism for the improvement will be investigated.

A. The effect of Xe contents variation

As He gas is added to the Ne–Xe gas mixture at a fixed Xe partial pressure and total pressure, the mobilities of Ne and Xe ions increase and that of He ions decreases because the collision cross-section of He ions is smaller than those of Ne and Xe ions, which can be obtained by the Blanc's law[11] as shown in Fig. 3. The ion mobility is proportional to the mean free path of ion momentum transfer and the collision sheath width at the cathode. Thus, as the ion mobility increases, the electric field at the cathode sheath is weakened.[2] The changes in the ion mobilities affect the vuv efficacy.

Figure 4 shows the potential profiles in the PDP cell for each gas and each gap conditions at the peak of the discharge current. Figure 4(a) shows that most of the potential drop is occurring within the cathode sheath region in the Ne–Xe gas mixture. As the He mixing ratio increases, the potential drop within the cathode sheath region decreases and the cathode sheath width increases. The decrease in the potential is due to the decrease in the ionization rate with increasing He mixing ratio and the increase in cathode sheath width is due to the increase in the ion mobility caused by He addition as shown in Fig. 3(a). These effects of the He addition cause the
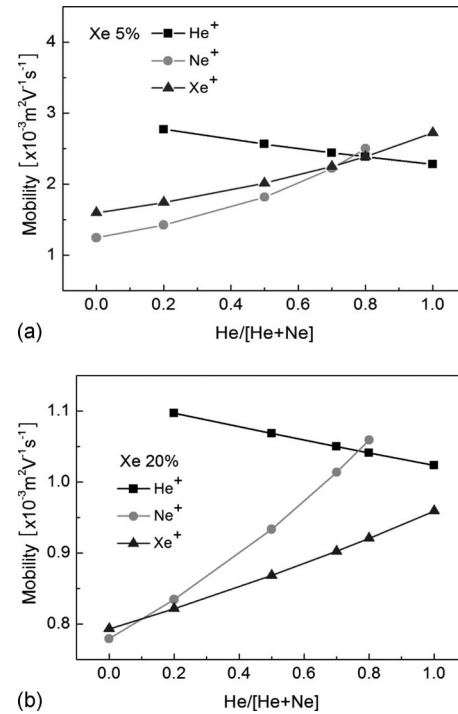
electric field at the cathode sheath to decrease and therefore, it is expected that the ion heating through the cathode sheath at 5% Xe content decreases with increasing He mixing ratio. Potential profiles at 20% Xe content are shown in Fig. 4(b). Potential drops occur mostly within the cathode sheath region in the Ne–Xe gas mixture, as in the case of 5% Xe content. However, the decrease in potential at the cathode sheath with He addition does not occur as a result of the low ion mobility at high Xe content. As shown in Fig. 3(b), the Xe ion mobility at 20% Xe content is smaller than that at 5%, and the increase in Xe ion mobility at 20% Xe content with increasing He mixing ratio is also smaller. He addition at 20% Xe content is less effective in reducing the ion heating caused by the lower rate of decrease in the electric field strength at the cathode sheath.

Figure 5 shows the time-averaged power delivered to electrons at unit volume during the pulse-on time for each gas and each gap condition. The electron heating in the Ne–Xe gas mixture occurs at the cathode sheath at both 5% and 20% Xe content. As the He mixing ratio increases, the region of the highest electron heating at 5% Xe content moves from the cathode sheath to the gap space, but the highest electron heating at 20% Xe is still at the cathode sheath. At 5% Xe, as shown by Fig. 5(a), the decrease in the electric field at the cathode sheath with the He addition is insufficient to increase the electron heating. Electrons need to travel along a path longer than the cathode sheath width in order to compensate for the insufficient power gain. The region of the highest electron heating at high He mixing ratios occurs at the gap space, and the magnitude in the region is quite smaller than that at low He mixing ratios. The lowered cathode sheath field is beneficial to increasing the Xe excitation. As the maximum electron heating region moves to-
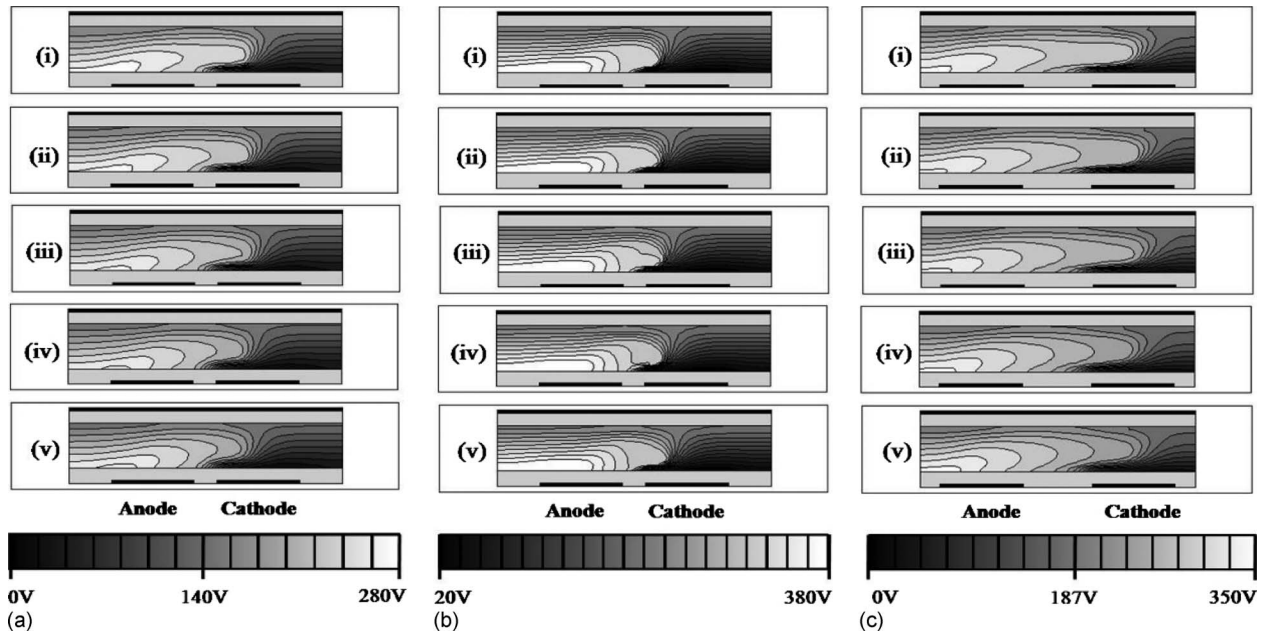
FIG. 4. Potential profile at increasing He mixing ratios at the discharge current peak time. (a) 5% Xe content and 60 μm electrode gap, (b) 20% Xe content and 60 μm electrode gap, and (c) 5% Xe content and 200 μm electrode gap. He/(He+Ne)=(i) 0, (ii) 0.2, (iii) 0.5, (iv) 0.8, and (v) 1.

ward the gap space, electron power is mostly consumed by the Xe excitation since electron powers gained at the gap space is insufficient to ionize neutral atoms. But at 20% Xe content case, as the He mixing ratio increases, the maximum electron heating region is still in the cathode sheath and the magnitude decreases. The decrease in the electron heating at the cathode sheath is so small and the region of the electron heating locally at the gap space is so broad that the increase in the electron heating at the gap space compensates for the reduced the electron heating at the cathode sheath. Since Xe atom has a low ionization energy, a large fraction of electron power can be used for the ionization of Xe atoms and not for the excitation.

Both the cathode sheath field and the electron heating affect the vuv efficacy directly. Cathode sheath field delivers power to electrons and ions. The vuv efficacy is proportional to the product of the electron heating efficacy ρ_1 and the Xe excitation efficacy ρ_2.[2] The electron heating efficacy ρ_1 is the ratio of the power delivered to electrons to the total input power and the Xe excitation efficacy ρ_2 is the ratio of the power consumed by Xe excitation to the power delivered to electrons. Figure 6 shows the incremental ratio of the power delivered to electrons and ions and consumed by excited Xe species with increasing He mixing ratio for each gas and each gap condition. The incremental ratio here means the ratio of the power delivered to each species with He added
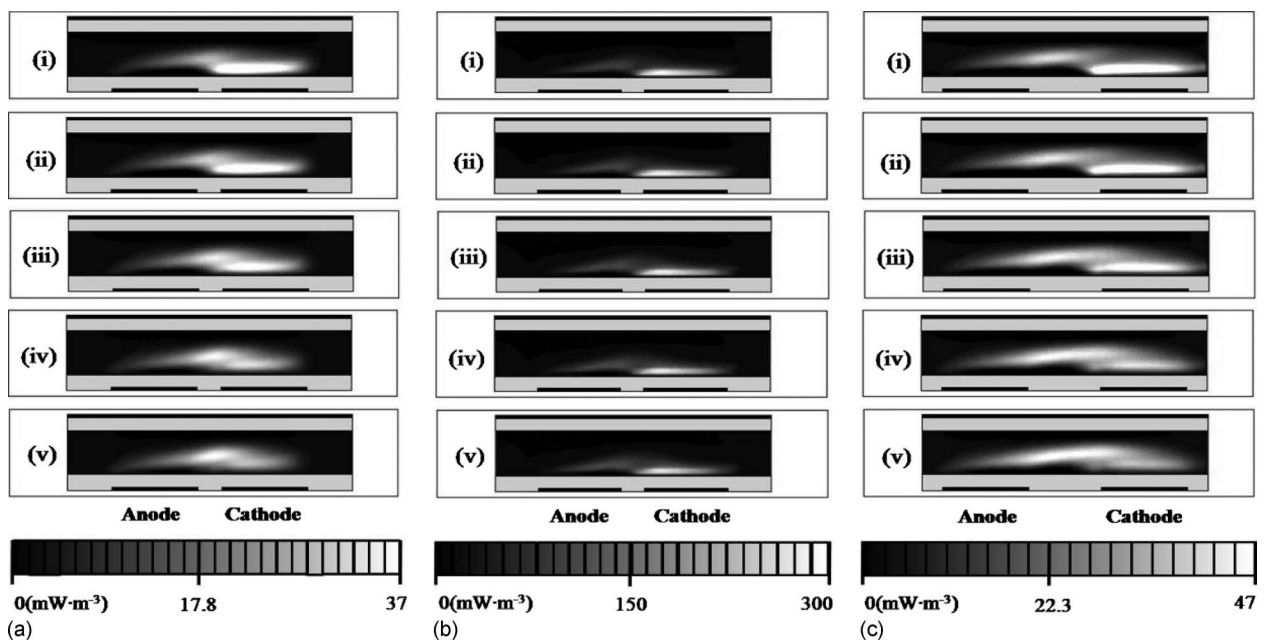

FIG. 5. Time-averaged power delivered to electrons in unit cell during the pulse-on time in (a) 5% Xe content and 60 μm electrode gap, (b) 20% Xe content and 60 μm electrode gap, and (c) 5% Xe content and 200 μm electrode gap. He/(He+Ne)=(i) 0, (ii) 0.2, (iii) 0.5, (iv) 0.8, and (v) 1.
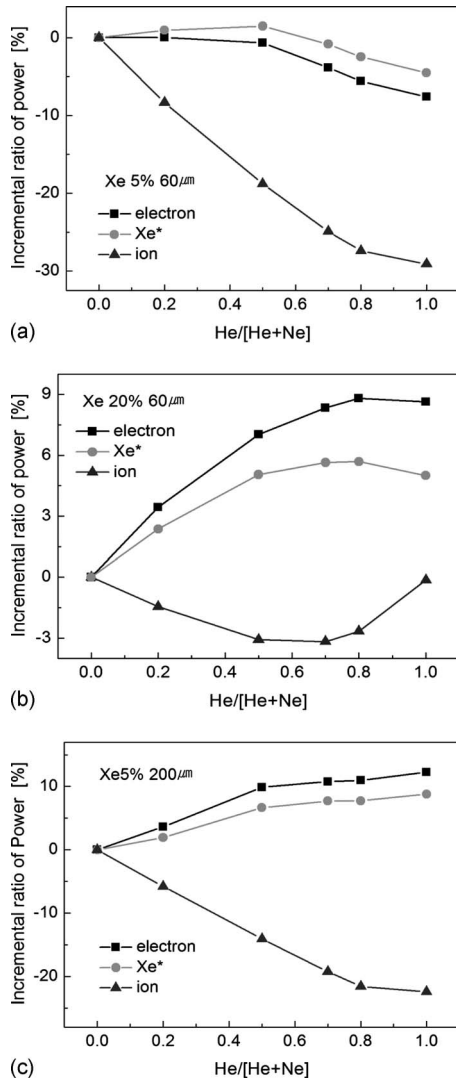
FIG. 6. Incremental ratio of power delivered to electrons and ions and consumed by excited Xe species at increasing He mixing ratios (a) 5% Xe content and 60 μm electrode gap, (b) 20% Xe content and 60 μm electrode gap, and (c) 5% Xe content and 200 μm electrode gap.

FIG. 7. Two partial efficacies ρ_1 and ρ_2 at increasing He mixing ratios (a) 5% Xe content and 60 μm electrode gap, (b) 20% Xe content and 60 μm electrode gap, and (c) 5% Xe content and 200 μm electrode gap.

gas mixture to the power delivered to each species with only Ne–Xe gas mixture. The negative incremental ratio of the power means that the power delivered to the species in a certain gas condition is lower than that in only Ne–Xe gas mixture.

Figure 6(a) shows that the powers delivered to the three species at 5% Xe content decreases with increasing He mixing ratio. The decrease in the electric field at the cathode sheath with the He addition causes a decrease in the electron heating, ion heating and excitation of Xe atoms. Therefore, the decrease in the amount of the power consumed by Xe excitation is smaller than that for other species. The reason for the decreased rate of power delivered to electrons than ions at high He mixing ratios is due to the electron heating at the gap space at high He mixing ratios. The electron heating at the gap space prevents the total power delivered to electrons from decreasing abruptly. When the He mixing ratio is increased, the steep decrease in the ion heating causes ρ_1 to increase, and the decrease in the cathode sheath field and the power delivered to electrons cause ρ_2 to increase, as shown
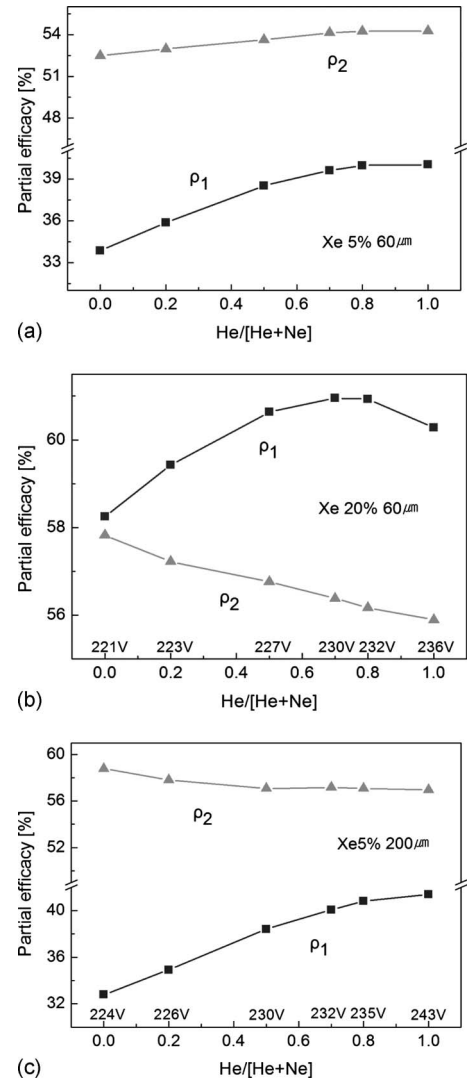
in Fig. 7(a). ρ_2 shows a much higher value than ρ_1, but the increase in the rate of ρ_2 is smaller than that of ρ_1. Therefore ρ_1 is the dominant factor in increasing the vuv efficacy with increasing He mixing ratio at 5% Xe content.

Figure 6(b) shows that the powers delivered to electrons and consumed by Xe excitation at 20% Xe content increases with increasing He mixing ratio, but the powers delivered to ions decreases first and then increases after the He mixing ratio of 0.7. As the He mixing ratio increases, the small decrease in the cathode sheath field and the increase in the electron heating locally at the gap space contribute to increasing the total power delivered to electrons compared with that in the usual Ne–Xe gas mixture. The increase in the amount of power consumed by Xe excitation is smaller than the increase in the power delivered to electrons since the increased electron heating causes electrons to consume their energy for the ionization of Xe atoms instead of the excitation of Xe. The decrease in the amount of the power delivered to ions before the He mixing ratio of 0.7 is much smaller compared with that at 5% Xe content since the decrease in the amount of cathode sheath field at 20% Xe con-
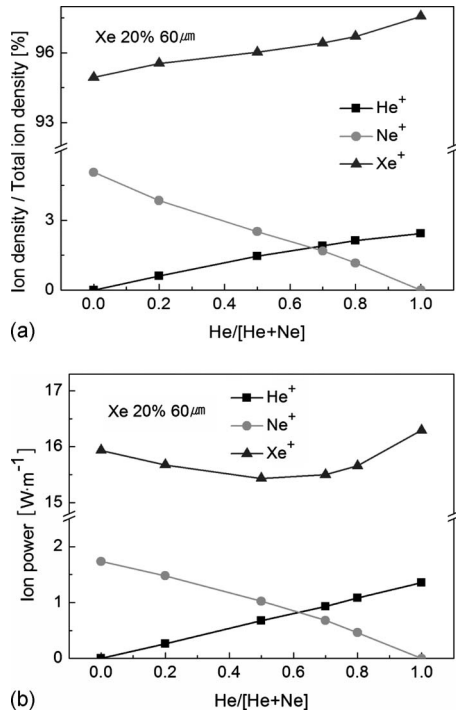
FIG. 8. (a) Ratio of each ion density to the total ion density at increasing He mixing ratios at 20% Xe content and 60 μm electrode gap. (b) Power delivered to each ion species at increasing He mixing ratios at 20% Xe content and 60 μm electrode gap.

tent is small. After the He mixing ratio of 0.7, the power delivered to ions increases and the amount of power is related to the increase in the ratio of Xe ion density to total ion density.

Figure 8(a) shows the ratio of each ion density to total ion density at increasing He mixing ratios. Before the He mixing ratio reaches 0.7, the ion species in the discharge space mostly consists of Xe and Ne ions. The decrease in the ionization at the low potential position in the cathode sheath region can be attributed to the lower ionization energy of Xe and Ne compared to that of He, and ion heating can be attributed to ions' traveling along the short path until the He mixing ratio of 0.7. However, since the decreased cathode sheath field is insufficient to ionize He atoms after the He mixing ratio reaches 0.7, the ionization of Xe atoms increases more in spite of increasing absolute amount of He gas. As shown in Fig. 8(a), the rate of increase in the Xe ion density ratio after the He mixing ratio of 0.7 is twice higher than before the He mixing ratio of 0.7. Although the much-lowered cathode sheath field with He addition at 5% Xe content contributes to the decrease in the ion heating caused by the increased mobility of Xe ions, the cathode sheath field generated at 20% Xe content is still high and the ionization of Xe increases; consequently, Xe ion heating increases as shown in Fig. 8(b), and the total ion heating increases with increasing He mixing ratio. Therefore, ρ_1 increases until the He mixing ratio reaches 0.7 but decreases thereafter, and ρ_2 decreases with increasing He mixing ratio as shown Fig. 7(b). ρ_1 and the increased rate of ρ_1 are larger than ρ_2 so that the increase in ρ_1 causes the vuv efficacy to increase before

the He mixing ratio of 0.7. However, the decrease in ρ_1 causes a decrease in the vuv efficacy after the He mixing ratio of 0.7.

B. The effect of sustain electrode gap length variation

The changes in discharge characteristics in the He–Ne–Xe gas mixture with varying sustain electrode gap lengths are analyzed at the fixed Xe partial pressure of 5%. Figure 4(c) shows the potential profile at the 200 μm electrode gap. Compared with the potential profile at the 60 μm electrode gap, the decrease in the cathode sheath field is similar, but the electric field at the gap space increases more in the case of the 200 μm electrode gap. The decrease in the cathode sheath field with the addition of He is due to the increase in the ion mobility as in the 60 μm electrode gap condition. Most ionization is caused by the cathode sheath field, and it is expected that ion heating also decreases. However, since electrons travel to the anode electrode, the increased electric field at the gap space can make the electron heating increase.

Figure 5(c) shows the time-averaged power delivered to electrons per unit volume during the pulse-on time under the 200 μm electrode gap conditions. Electrons are heated at the cathode sheath and the gap space simultaneously until the He mixing ratio reaches 0.5. With increasing He mixing ratios, the potential difference from the end of the cathode sheath to the edge of the anode electrode increases, and the increased electric field at the gap space contributes to heating electrons. After the He mixing ratio reaches 0.5, the region of the highest electron heating moves from the cathode sheath to the gap space as in the 60 μm electrode gap condition. Under the 60 μm electrode gap condition, although the electric field at the gap space increases, the power delivered to electrons at the gap space is low due to a insufficient distance to heat electrons. The decrease in the amount of the power delivered to electrons at the cathode sheath is replenished with the heating caused by the increasing electric field at the gap space after the He mixing ratio of 0.5; the long gap is sufficient to increase the electron heating. Therefore, the power delivered to ions decreases and the power delivered to electrons increases as shown by Fig. 6(c). The increase in the amount of the power consumed by the Xe excitation is smaller than that of the power delivered to electrons. The fraction of the excited Xe decreases due to the electron heating at the gap space.

With increasing He mixing ratios, the increase in the electron heating at the gap space causes ρ_1 to increase, and the increase in the power delivered to electrons causes ρ_2 to decrease as shown by Fig. 7(c). Although ρ_2 shows much higher value than ρ_1 as in the 60 μm electrode gap condition, ρ_2 decreases and ρ_1 increases so that ρ_1 is also the dominant factor in increasing the vuv efficacy with increasing He mixing ratios at 200 μm electrode gap.

III. CONCLUSION

The changes in the vuv efficacy with the addition of He to the Ne–Xe gas mixture in the PDP are analyzed via a

two-dimensional numerical simulation. When the sustain electrode gap is fixed at 60 μm and Xe content is changed, He addition at the low Xe content of 5% causes a decrease in the ion heating due to the decrease in the cathode sheath field. However, as the Xe content is increased to 20%, the vuv efficacy increases until the He mixing ratio of 0.7 due to the increase in the electron heating. Beyond the He mixing ratio of 0.7, an increase in Xe ion heating causes the vuv efficacy to decrease. When the Xe content is fixed at 5% and the sustain electrode gap is changed to 200 μm, the vuv efficacy increases due to the increase in electron heating at the gap space at increasing He mixing ratios. It is found that the continuous improvement of the vuv efficacy at increasing He mixing ratios takes place for the gas mixture with the low Xe content of 5% regardless of the sustain electrode gap, while the efficacy improves only up to the He mixing ratio of 0.7 for the mixture with the high Xe content of 20%.

[1] G. Oversluizen, M. Klein, S. de Zwart, S. van Heusden, and T. Dekker, J. Appl. Phys. **91**, 2403 (2002).

[2] W. J. Chung, B. J. Shin, T. J. Kim, H. S. Bae, J. H. Seo, and K.-W. Whang, IEEE Trans. Plasma Sci. **31**, 1038 (2003).

[3] H. S. Bae, W. J. Chung, and K.-W. Whang, J. Appl. Phys. **95**, 30 (2004).

[4] K. C. Choi, N. H. Shin, K. S. Lee, B. J. Shin, and S.-E. Lee, IEEE Trans. Plasma Sci. **34**, 385 (2006).

[5] H. S. Bae, J. K. Kim, and K.-W. Whang, IEEE Trans. Plasma Sci. **35**, 467 (2007).

[6] J. H. Seo, H. S. Jeong, J. Y. Lee, C. K. Yoon, J. K. Kim, and K.-W. Whang, J. Appl. Phys. **88**, 1257 (2000).

[7] I. Lee and K. Y. Choi, J. Appl. Phys. **96**, 1829 (2004).

[8] J. H. Seo, W. J. Chung, C. K. Yoon, J. K. Kim, and K.-W. Whang, IEEE Trans. Plasma Sci. **29**, 824 (2001).

[9] S. K. Lee, J. H. Kim, J. Lee, and K.-W. Whang, Thin Solid Films **435**, 69 (2003).

[10] H. J. Lee, D.-K. Lee, J.-H. Choi, Y.-S. Cho, H.-D. Park, H.-J. Lee, and C.-H. Park, Proceedings of the 2005 International Meeting on Information Display, 2005 (unpublished), p. 171.

[11] J. Meunier, Ph. Belenguer, and J. P. Boeuf, J. Appl. Phys. **78**, 731 (1995).